

Chapter 13

Effect of Organoclay on the Physical Properties of UV-Curable Coatings

Funda Inceoglu, Cahit Dalgicdir, and Yusuf Z. Menciloglu

Faculty of Engineering and Natural Sciences, Material Science and Engineering Program, Sabanci University, 34956 Orhanli, Tuzla, Istanbul, Turkey

The combination of UV-curing and nanocomposite technology has been studied to produce cost-effective coatings with superior physical and mechanical properties. The clay was modified with dimethyl dihydrogenated-tallow quaternary ammonium salt and made organophilic. The effect of the organoclay(2-10 phr) on curing rate, mechanical, thermal and physical properties of a urethane-acrylate coating has been determined. X-ray diffraction analysis, AFM, SEM and TEM images as well as the tensile properties of different formulations have confirmed the uniform distribution of organoclay in polymer matrix. At 3 phr organoclay addition, the UV-cured film exhibited the best mechanical performance due to the formation of both intercalated and exfoliated morphologies. Curing time was reduced and the initial thermal decomposition temperature shifted 50°C to higher temperature by the incorporation of small amount of organoclay. The nanocomposite coating was also found to be more resistant against scratching compared with clay-free coating.

Introduction

There is a growing interest today in polymeric nanocomposites because of the superior properties of this type of material. The layered smectite clay like montmorillonite is the most common type of inorganic filler for the preparation of such nanocomposites because the starting clay materials are easily available and they usually exhibit remarkable improvements in material properties when compared to virgin polymer or conventional microcomposites. Several studies have indicated that the addition of a few percentage of layered silicates resulted in enhanced mechanical, thermal, and barrier properties of the polymeric matrix material(1-5). The main reasons for these improvements are the clay layer thickness, which is on the order of 1 nm and very high aspect ratios (e.g. 10-1000). Therefore, when the clay layers are properly dispersed throughout the matrix with the possible mechanisms of intercalation and/or exfoliation, a few weight percent of clay creates a much higher surface area for polymer-filler interactions than do conventional composites. In order to achieve the good dispersion and thus enhanced properties, molecular structure of the silicate filler should be adjusted for the polymer used; otherwise phase separation may prevent nano-sized dispersion and lead to the formation of micron-sized agglomerates. The effect of adjustment includes the attenuation of adhesive forces between the silicate layers by the addition of alkyl ammonium salts. The resulting clay is known as organoclay(6).

The UV-curing process is used commonly for applications in the coating and ink industries because of its many advantageous properties offered. Among these benefits, the ultra-fast, solvent-free, ambient temperature curing are the most important ones which lead to an energy-saving up to 70%. The formulations for UV-curing process have three essential components: photoinitiator, oligomer or prepolymer, and reactive diluents. A photoinitiator is necessary to generate free radicals that will attack the double bond of the oligomer and start the chain reaction. There are several types of oligomers; the most commonly used are epoxy acrylates, urethane acrylates, unsaturated polyesters, polyester acrylates, and polyether acrylates(7-14). The wide use of urethane acrylates is due to their versatile chemistry that offers many different possibilities to the formulator. In this work, an aromatic urethane diacrylate was used. Generally, an aromatic urethane diacrylate gives good hardness, toughness, water resistance and gloss retention and it is used in applications like clear coating for paper, screen and metal decorating inks and coatings for rigid and flexible plastics. Reactive diluents are functional monomers that are used to adjust the properties of the solution like the viscosity. They are also added to regulate the volatility, odor, and solubility of the resulting films.

Recently, the UV-curable nanocomposite coating systems have attracted great attention due to their combined advantageous of both superior mechanical

properties and cost effective preparation technique(15-23). Decker et al. first demonstrated the preparation of UV curable acrylate-bentonite nanocomposite materials and suggested that an exfoliated structure was formed in the formula containing organoclay as evidenced by the absence of a X-ray diffraction (XRD) peak. They also observed higher transparency in the nanocomposite compared to the microcomposite obtained with the untreated bentonite(15). Benfarhi et al. synthesized different types of nanocomposite materials by photo-initiated crosslinking polymerization of epoxy, vinyl ether and acrylate-based resins containing 3 wt % of an organoclay(16). They showed that the glass transition temperature (T_g) of nanocomposites was lower and the materials were more flexible than the corresponding microcomposites obtained with untreated clay. The incorporation of silicate nanoparticles was also found to cause a severe drop of the gloss of the UV-cured polymers. Keller et al. examined the preparation and performance of polymer nanocomposites made of organoclay and a UV-cured polyurethane-acrylate(17). The nanocomposite materials exhibited superior tensile strength and elongation at break but the addition of clay or organoclay had hardly any effect on Young's Modulus and on T_g values. They also reported a significant reduction on gloss values of UV-cured coatings with the addition of organoclay and attributed this observation to an increase in surface roughness upon the addition of the clay nanoparticles. Shemper et al. investigated the effect of synthetic clay (Laponite) on the photo-polymerization kinetics of methyl α -hydroxymethylacrylate (MHMA) systems and suggested that, in the presence of clay, earlier onset of autoacceleration was observed, higher rates of polymerization were achieved, and high final overall conversions were reached(18). Higher rates and increase in conversions were also realized as the clay content increased in the medium. Similar results were also reported by Uhl et al. in their studies related with UV-curable urethane acrylate films containing organoclay(19). Decker et al. have developed a novel method to synthesize highly resistant nanocomposite polymers by photo-initiated polymerization of multifunctional acrylate or epoxy monomers containing small amounts (3 wt%) of an organoclay(20). The highly crosslinked nanocomposite polymers were found to be quite resistant to organic solvents, moisture and weathering, as well as to scratching. The loss of gloss was attributed to a surface roughness created by the clay nanoparticles. The nanocomposite surface was reported to be less slippery due to the increased roughness. Fogelstrom et al. prepared nanocomposites from the hyperbranched polyester Boltorn H30, acrylated to 30% and 70%, and modified Na^+ -montmorillonite(21). They revealed that films prepared from 30% acrylated Boltorn H30 with clay added after the acrylation exhibited a harder surface, better scratch resistance, better adhesion to metal substrates and a small increase in flexibility. Uhl, et al. studied the structure and properties of UV curable epoxy acrylate films reinforced with nanoclay(22). The intercalated structures were observed and the mechanical

properties were found to be improved for all films containing modified or unmodified clay. It was suggested that property enhancements were not only dependent upon the nanoclay but the structure of the polymer and how the two interact. Tensile strength, Young's Modulus and elongation at break showed increases up to about 50%, 50% and 20%, respectively, due to the addition of various clays. In very recent work of Wang, et al., the preparation of a UV-curable intercalated/exfoliated nanocomposite resin that was applied to an organic light-emitting device (OLED) packaging was demonstrated(23). Better thermal stability, lifetime and moisture properties were observed in nanocomposite samples.

The present work investigates the effect of organoclay on mechanical, thermal, scratch resistance, and flame-retardant properties of UV-curable acrylate films. The structure-property relationship is discussed in a comprehensive manner. This study is also unique in illustrating the highest improvements, especially in mechanical properties of UV-curable acrylate resins, which were achieved up to now by using organically modified clays.

Experimental

Materials

Aromatic urethane diacrylate, supplied from UCB Chemicals (Belgium), was used as the oligomer matrix. 1,6-Hexanediol diacrylate (HDDA) and N-vinyl pyrrolidone (NVP) as reactive diluents were supplied by BASF (Germany). Trimethylol propane triacrylate (TMPTA) from UCB Chemicals was used as a cross-linker. The photoinitiator is 2,4,6 trimethyl benzoyl diphenyl phosphine oxide (TPO) and was supplied by Ciba Specialty Chemicals (Switzerland). Clay was obtained from Karakaya Company and modified with dimethyl dehydrogenated-tallow quaternary ammonium salt supplied by Kalekimya Company. The hydrogenated tallow consists of ~ 65% C18, ~30% C16 and ~5% C14 and the counterion is chloride.

Organoclay Preparation

40 g of bentonite having cation exchange capacity (CEC) of 64 meq/100 g was dispersed in deionized water and kept at room temperature until the red (ferric oxide) and white (calcium bentonite) precipitates have been observed. The upper part of the dispersion, which is rich in sodium bentonite with CEC of 104 meq/100 g (determined by methylene blue test), was then treated with dimethyl dihydrogenated-tallow quaternary ammonium salt for 6 hrs at 80°C.

The weight ratio of clay:quaternary salt was kept at 1:1. The organoclay was then filtered, washed with methanol and dried in an oven.

Coating Preparation

The liquid formulation of resin containing 45 wt % aromatic polyurethane diacrylate, 30 wt% HDDA, 10 wt % TMPTA, 10 wt % NVP and 5 wt % TPO was prepared for clay-free resin. The clay was dried in a vacuum oven at 120°C for 24 hours and then dispersed in the range between 2-10 phr (parts per hundred weight of resin) for preparing nanocomposite coating formulation. The solution was stirred at room temperature for half an hour and then put into ultrasonic bath for an hour in order to disperse the clay particles homogeneously in the resin. The liquid resin was then applied on glass plates and exposed to UV-radiation for 60 min. from a photoreactor consisting of eight TL 6W/08/F6T5 BLB-type UV lamps (6W, Phillips; The Netherlands).

Characterization

The progress of photo-polymerization was determined by gel content measurements. The weight loss after 48 hours of extraction in acetone using soxhlet apparatus was calculated for the determination of gel content. The level of interlayer separation of clay platelets were measured by X-ray diffraction (XRD) analysis conducted using a Bruker AXS-D8 diffractometer operating at 40kV and 40 mA. The mechanical properties of the coating films (at least 5 samples from each formula) were measured via Instron Model No. 5565 at a cross speed of 5 mm/min. A Netzsch DSC 204 was used to determine glass transition temperature(T_g) of the samples. The samples were cyclically heated and cooled from -50 to 200°C, using a heating rate of 5K/min. and cooling rate of 50K/min. For the morphology observations, Leo G34-Supra 35VP scanning electron microscope (SEM) was used. AFM images were taken using Digital Instruments NanoScope IIIa. Samples for TEM analysis was prepared using a Nova ultramicrotome equipped with a diamond knife and the sections were collected on formvar/carbon 300-mesh copper grids. The TEM micrographs were taken at an acceleration voltage of 200kV. The thermal properties of the films were analyzed using Netzsch STA 449C with a heating rate of 20 °C / min. under air atmosphere. The gloss measurements were conducted on a Minolta Multigloss 268. The effect of clay on the flame retardancy of the coatings was determined via home made limiting oxygen index (LOI) apparatus according to ASTM D 2863. Scratch testing was done by performing 50 double rubs using 0000 grade steel wool. The percentage of gloss values maintained after the scratch test was measured for both clay free and nanocomposite coatings. The

surfaces were analyzed by SEM to determine the depth and the number of the scratches formed.

Results and Discussion

In order to achieve layered dispersion of clay in polymeric matrix, the molecular structure of the filler should be adjusted for the polymer used. In the present study, this adjustment was achieved by exchanging alkali cations between the clay layers with alkyl ammonium salt. This treatment leads to the widening of the clay galleries, as shown by the shift of the peak belonging to d_{001} plane toward the smaller angles of x-ray diffraction pattern (Figure 1). The clay galleries were opened up from 1.2 nm to 1.9 and 3.3 nm after the treatment with alkyl ammonium salt. The peak of original clay at $2\theta = 7^\circ$ was still present in organoclay, but the intensity was very low. When organoclay was incorporated into the acrylate resins, the characteristic peaks at $2\theta = 7^\circ$ and $2\theta = 4.5^\circ$ completely disappeared from the spectrum for the samples with 2-7 phr organoclay, while the peak at $2\theta = 4.5^\circ$ was retained in sample with 10 phr filler. In all organoclay containing films, most of the clay galleries were opened up to 4.0 nm, indicating the highly intercalated morphology. The detector peak broadening at around $2\theta = 2.0^\circ$ for the sample containing 3 phr organoclay was attributed to the presence of both intercalated and exfoliated clay layers (Figure 2).

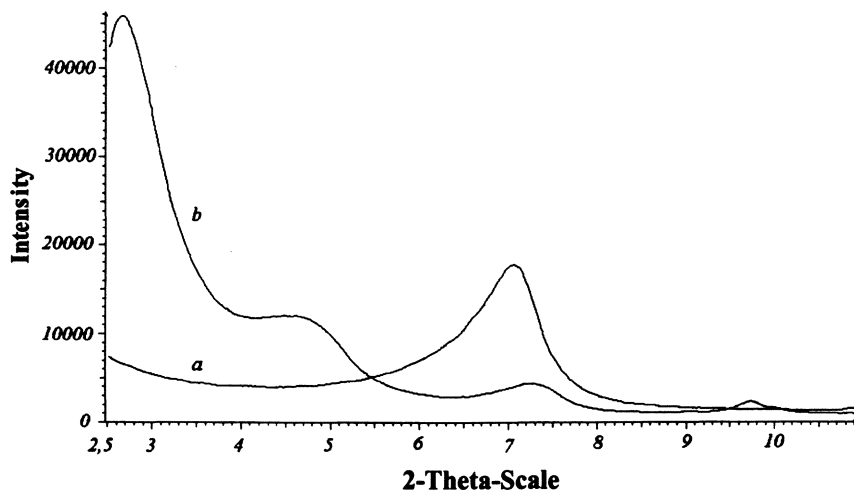


Figure 1. X-ray diffraction profile of (a) pure clay, (b) organoclay.

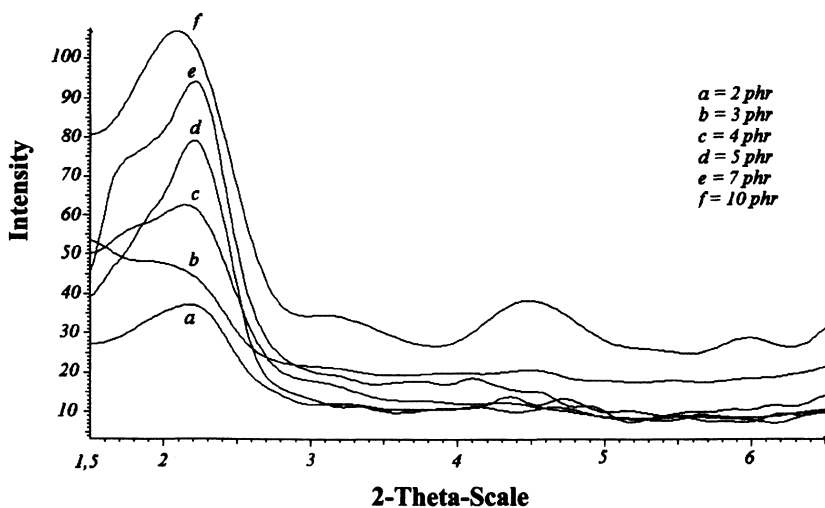


Figure 2. X-ray diffraction profile of nanocomposite films with 2-10 phr organoclay.

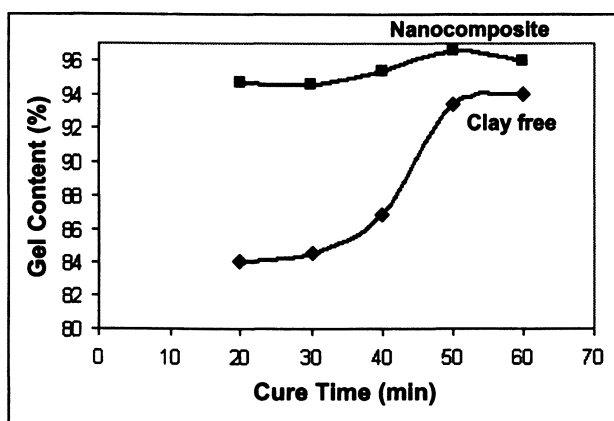


Figure 3. Gel content versus UV-radiation exposure time curves for clay-free and nanocomposite (3 phr organoclay) samples.

The effect of organoclay on the progress of polymerization was determined from the gel content measurements. Figure 3 shows gel content versus time graph for clay-free and nanocomposite films. It was observed that the gel content increased rapidly with the time of UV exposition for clay-free resin and reached a plateau at 50 minutes, after which the change was very little due to the mobility restriction upon gelation. The final gel content is 94% after 60 minutes of radiation. A faster polymerization was observed in nanocomposite films, reaching the same level of crosslink density at a shorter time of UV-radiation. This behavior can be attributed to two different mechanisms. First of all, strong interaction between polymer matrix and silicate layers may occur through the formation of hydrogen bonds which can act as a physical crosslink. Secondly, clay layers may reduce the rate of termination by inhibiting the mobility of polymer chains, resulting in increased rate of polymerization(12). The change in gel content was very low after 20 minutes of radiation in nanocomposite film.

Tensile strength, modulus and strain properties of UV-cured coating films as a function of organoclay content are given in Figure 4. These mechanical properties are closely related to the level of filler dispersion inside the polymer matrix. It can be seen that there is an increase in all the properties with the addition of organoclay. The properties are superior in nanocomposite films, even at 10 phr filler loading. The peak in tensile properties was attained with 3 phr organoclay addition. This observation is related with the layered dispersion and the optimum amount of reinforcing filler in that sample. It is known that each exfoliated layer behaves as single reinforcing filler and affects the tensile properties to a great extent.

In general, the elasticity of most of the thermoplastic materials decreases with the incorporation of inorganic filler. To the contrary, in thermoset films, the flexibility can be enhanced due to the plasticizing effect of long alkyl chains in quaternary ammonium salts(24,25). This effect seems to be much more significant in the nanocomposite film with 3 phr organoclay. We attribute this behavior to the presence of exfoliated clay layers since most of the long alkyl chains are in the polymeric matrix, and as a result, they are freer to move compared to intercalated morphology, in which they reside between the clay layers. This observation is consistent with the glass transition temperatures (T_g) of the films, determined from DSC analysis (Figures 5 and 6). The lowest T_g value belongs to the nanocomposite film with 3 phr organoclay because of the presence of dangling chains with higher degree of freedom that contribute to better flexibility.

Scanning electron microscopy (SEM) and atomic force microscopy (AFM) are the valuable tools to study the dispersion level of fillers in polymer matrix. Figures 7 and 8 illustrate SEM and AFM images of nanocomposite films, respectively. In addition to nano-sized clay particles, small amount of agglomerates were also observed by SEM in the samples containing 5 and 10 phr organoclay. It was not easy to produce a good image from 3 phr organoclay loaded film due to very fine,

layered dispersion. Thus, AFM analysis was conducted to see the dispersion of clay platelets in this sample. The images have confirmed the presence of finely distributed clay platelets in acrylate resin without the formation of any clay agglomerates (Figure 8).

Transmission electron microscopy (TEM) was used to further investigate the nanocomposite structures. Figure 9 shows the TEM micrographs of the sample containing 3 phr organoclay. The micrographs confirmed the homogeneous dispersion of clay layers and the presence of both intercalated and exfoliated morphologies. The d-spacing of clay layers in intercalated structure, which is about 4 nm, corroborates the XRD results given in Figure 2. In the case of nanocomposite sample with 5 phr organoclay, only intercalated morphology was observed with the d-spacing of between 2.8 and 4.2 nm (Figure 10). There were also some clay agglomerates in the sample as they were previously observed in the SEM images (see Figures 7a and 10).

Thermal stability and decomposition behavior of various crosslinked coatings were determined by thermogravimetric analysis (Figure 11). The initial decomposition temperature shifted 50°C to higher temperature with the addition of only 2 phr organoclay. The initial thermal stability is related to the homogeneous distribution of the clay layers throughout the matrix. Each layer in the matrix behaves like a thermal insulation layer and increases the path length of the volatile products. Further addition of filler affected the thermal stability only little compared to that of 2 phr that was attributed to the presence of sufficient barrier layer at this filler content. The decomposition occurred in two steps for neat resin; the main decomposition of the sample took place between 220°C and 400°C and the further decomposition of the macromolecules, formed in the first stage, was observed at temperatures higher than 400 °C. In nanocomposite samples, the decomposition occurred in a single step due to the delayed first decomposition.

The change in char yield with organoclay can be seen in Table 1. The percent change in char yield was larger than the amount of organoclay added, confirming the char promoting effect of the filler. The char yield was not affected much from the organoclay content after 3 phr. This is probably due to the sufficient amount of clay layers acting as thermal insulators at this filler content.

The effect of organoclay on flame retardancy was evaluated by limiting oxygen index (LOI) test method and the results are given in Table 1. It is known that clay cannot stop burning of the polymers by itself, but it decreases the generation of toxic gases, delays the ignition and provides a heat barrier. In our system, the minimum oxygen amount in the mixture of nitrogen and oxygen gases just needed to support the flame of ignition was found to increase from 19% to 20% by the incorporation of 2 phr organoclay. The effect of further addition of filler on flame retardancy was not detectable. This behavior is consistent with the thermal stability results and further indicates the present of sufficient amount of clay layers acting as thermal insulators at this level of filler content.

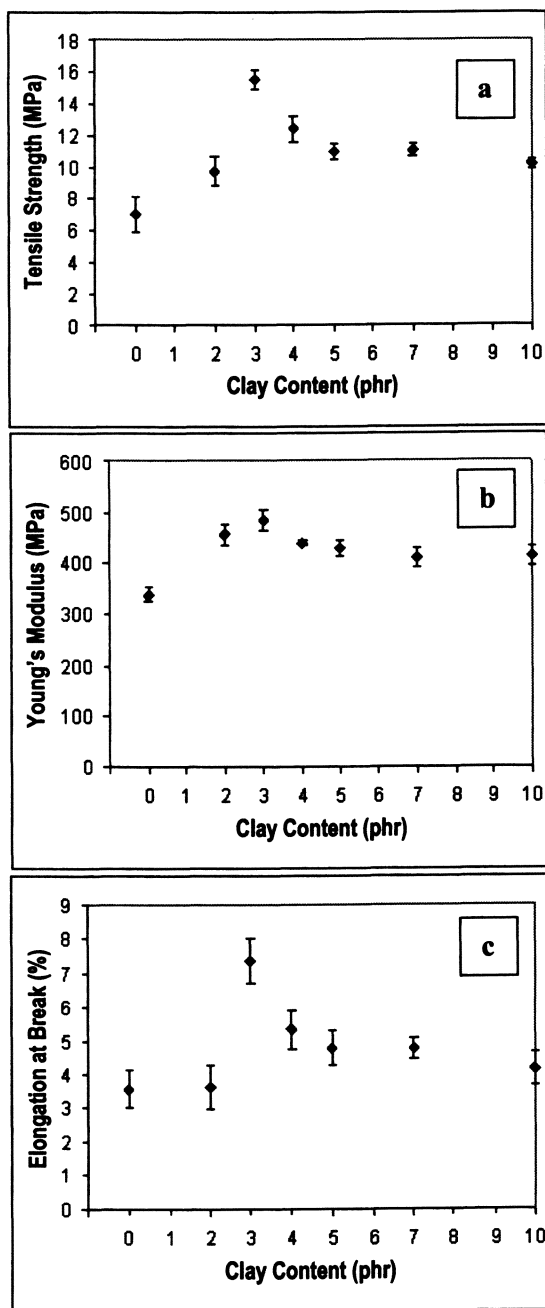


Figure 4. Tensile properties of acrylate films as a function of organoclay content: (a) Tensile Strength; (b) Young's Modulus; (c) Elongation at Break.

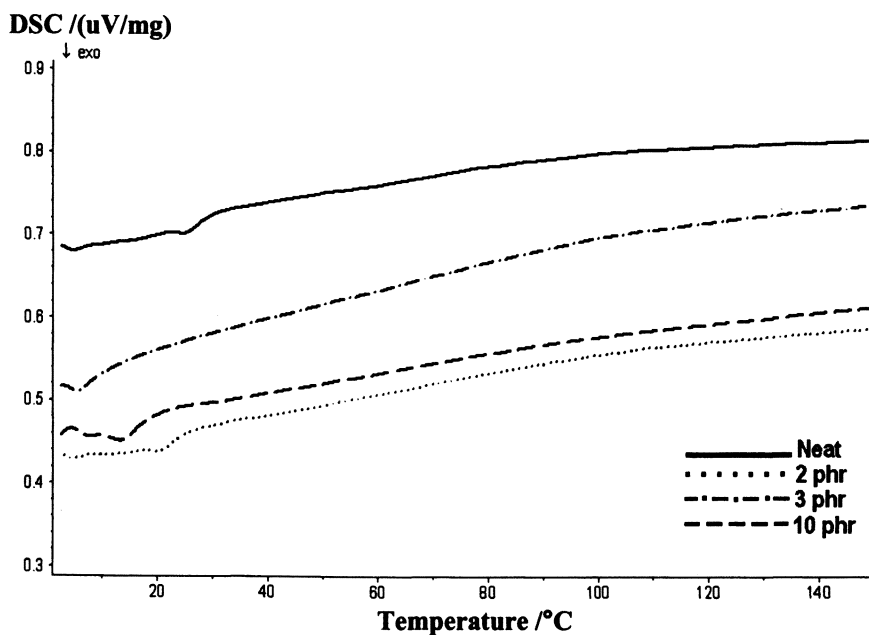


Figure 5. DSC thermograms of neat and organoclay containing acrylate samples.

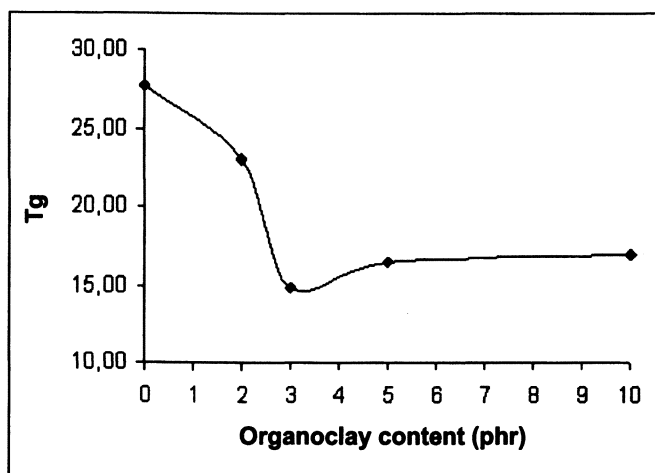


Figure 6. Change in T_g of acrylate samples with organoclay content

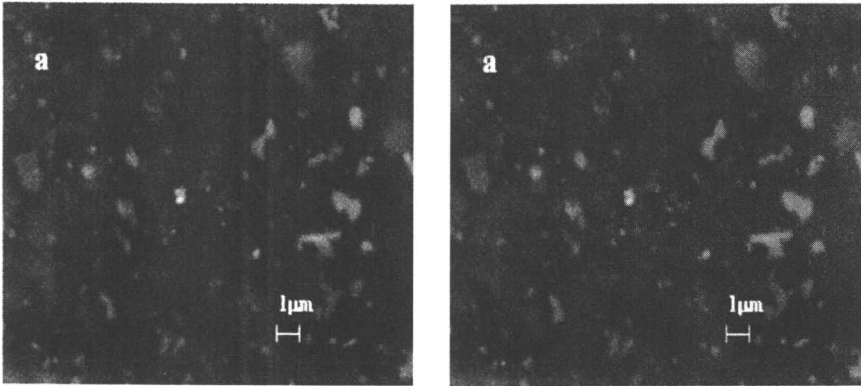


Figure 7. SEM images of acrylate samples having (a) 5 phr, (b) 10 phr, of organoclay.

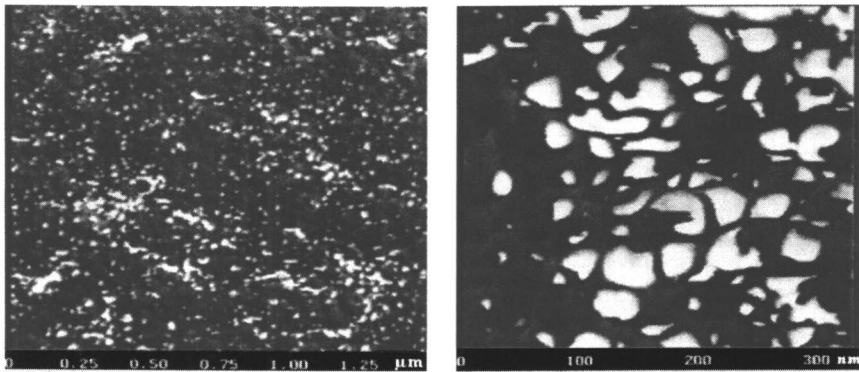


Figure 8. AFM images of nanocomposite sample with 3 phr organoclay

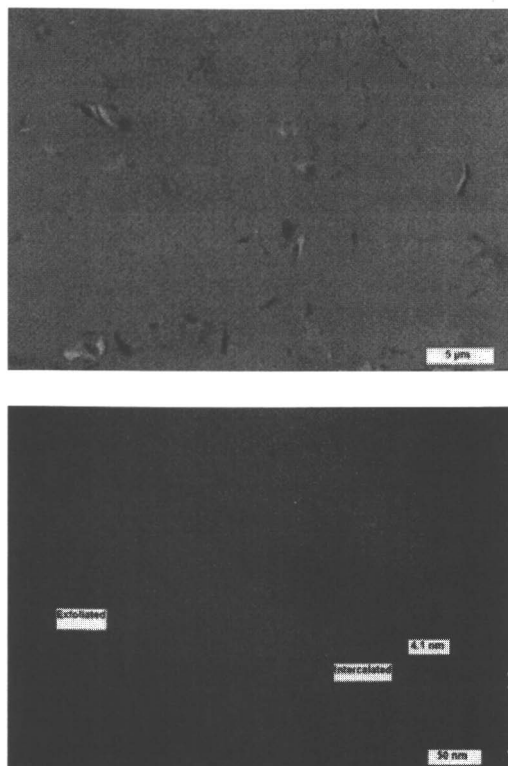


Figure 9. Transmission electron micrographs of acrylate nanocomposites with 3 phr organoclay.

In order to investigate the surface properties of the samples, gloss and abrasion resistance measurements were performed. It can be clearly seen that addition of organoclay as small as 2 phr sharply reduces the gloss of the UV-cured coatings (Table 2). The inorganic fillers usually creates surface roughness and this results in a significant amount of light to be dispersed rather than reflected from the surface. This matting effect of clay is desired for some applications like wood furniture and floor finishes(3). It is advantageous that clay can provide this at a lower level of loading than the conventional matting agents.

Resistance of the coatings to abrasion was determined by taking SEM images and measuring the gloss values after performing 50 cycles of steel wool abrasion test. The number and the width of the scratches are larger in clay-free sample when compared to the nanocomposite sample. To the contrary, the nanocomposite film surface exhibited less scratch damages (Figure 12). This can be related with the surface roughness created by nanofiller which contributes to

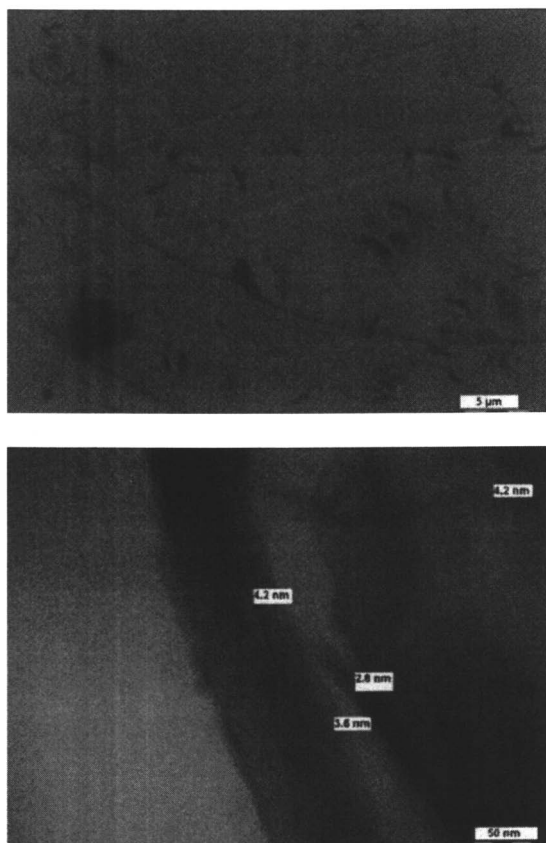


Figure 10. Transmission electron micrographs of acrylate nanocomposites with 5 phr organoclay.

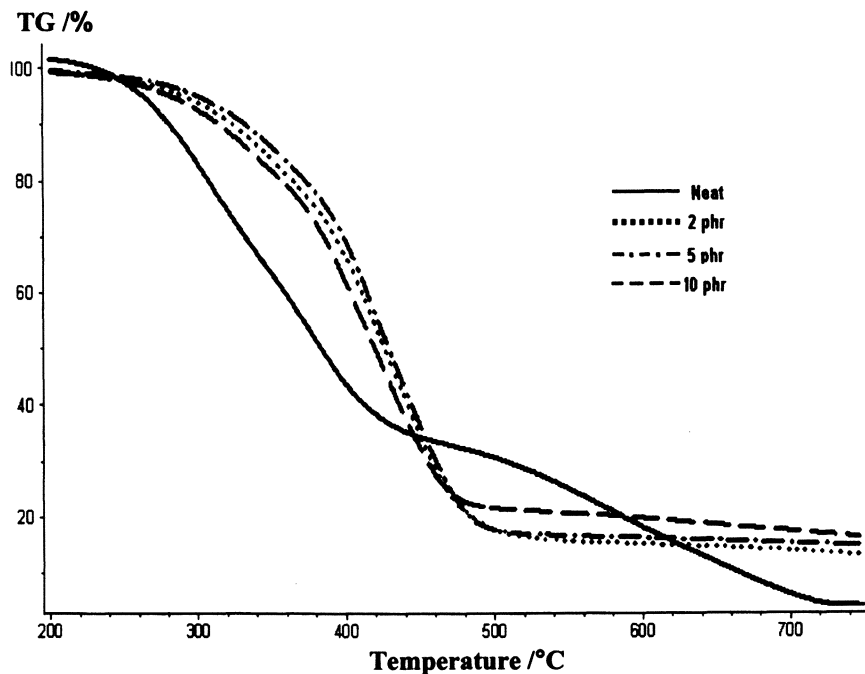


Figure 11. TGA of clay-free acrylate and acrylate nanocomposite coatings.

Table 1. Effect of organoclay content on char yield and limiting oxygen index (LOI).

<i>Organoclay Content (phr)</i>	<i>Char Yield (%)</i>	<i>LOI (%)</i>
0	4.51	19
2	10.66	20
3	12.27	20
4	12.91	20
5	13.74	20
7	14.51	20
10	14.45	20

Table 2. Influence of the clay content on the gloss* of acrylate coating films.

<i>Organoclay Content (phr)</i>	<i>20° Gloss Normalized (%)</i>
0	100
2	52
3	58
4	36
5	27
7	16
10	17

* Gloss measurements were made according to ASTM D523.

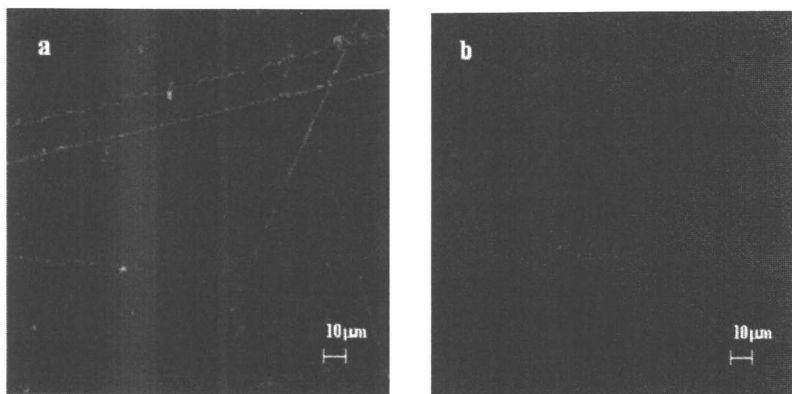


Figure 12. SEM images of (a) clay-free film surface, (b) nanocomposite with 3 phr organoclay film surface, following steel-wool scratch resistance test.

less contact area between the sample surface and the abrasive material. The scratch resistant characteristic of organoclay is also evident from the improvement in gloss retention of acrylate coating following the abrasion test (Figure 13).

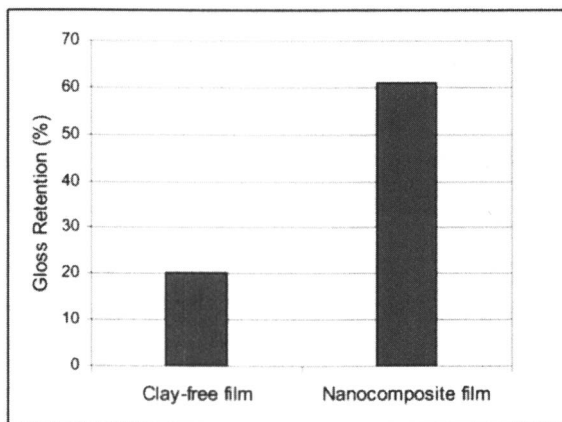


Figure 13. Gloss retention of the sample surfaces after steel-wool scratch resistance test.

Conclusions

The urethane-acrylate based nanocomposite coatings with different amounts of organoclay have been prepared by photoinitiated polymerization technique. Gel content measurements were performed in order to determine the effect of filler on crosslink density. It was found that using organoclay as reinforcing filler shortens the time required for the complete curing. X-ray diffraction studies as well as AFM and TEM images revealed that 3 phr organoclay was uniformly dispersed in the polymer matrix and both intercalated and exfoliated morphologies were present. In the case of acrylate samples with organoclay content higher than 3 phr, intercalated morphology as well as some clay agglomerates were observed. The most significant change in tensile properties and glass transition temperature of urethane-acrylate coating has occurred at 3 phr organoclay loading due to the layered dispersion of clay. The presence of organoclay was found to delay the initial decomposition of the matrix resin by increasing the path of volatile products, while it acted as a heat barrier and lead to the heat build-up at high temperature, thereby increased the char residue. Resistance to scratching was better in nanocomposite sample when compared to

clay-free one. Besides providing good mechanical and physical properties, organoclay appears to be a cost effective matting agent, small amount of which is sufficient to reduce the gloss significantly.

Acknowledgements

The authors would like to acknowledge the financial support of Sabanci University Research Foundation. They also want to thank Attila Alkan and Mehmet Ali Gulgun for their very valuable contributions in TEM analysis and also to Baran Inceoglu for his valuable helps throughout the study.

References

1. Gopakumar, T.G. Lee, J.A. Kontopoulou, M. Parent, J.S. *Polymer* **2002**, *43*, 5483-5491.
2. Alexandre, M., Dubois, P., *Materials Science and Engineering* **2000**, *28*, 1-63.
3. Decker, C., Keller, L., Zahouily, K., Benfarhi, S., *Polymer* **2005**, *46*, 6640-6648.
4. Nigam, V., Setua, D. K., Mathur, G. N., Kar, K.K, *Journal of Applied Polymer Science* **2004**, *93*, 2201-2210.
5. Zou, K., Soucek, M.D., *Macromolecular Chemistry and Physics* **2004**, *205*, 2032-2039.
6. Ray, S.S., Okamoto, M., *Progress in Polymer Science* **2003**, *28*, 1539-1641.
7. Studer, K., Nguyen, P.T., Decker, C., Beck, Schwalm, E. R., *Progress in Organic Coatings* **2005**, *54*, 230-239.
8. Chattopadhyay, D.K., Panda, S.S., Raju, K.V.S.N., *Progress in Organic Coatings* **2005**, *54*, 10-19.
9. Imamoglu, T, Yağci, Y, *Journal of Applied Polymer Science* **2002**, *83*, 1181-1189.
10. Ali, M. A., Khan, M.A., Idriss Ali, K. M., *Advances in Polymer Technology* **1998**, *17*, 259-267.
11. Asif, A., Shi, W., *Polymers for Advanced Technologies* **2004**, *15*, 669-675.
12. Inceoglu, A.B., Yilmazer, U., *Polymer Engineering and Science* **2003**, *43*, 661-669.
13. Uhl, F.M., Davuluri, S. P., Wong, S. C., Webster, D. C., *Chemistry of Materials* **2004**, *16*, 1135-1142.
14. Masson, F., Decker, C., Jaworek, T., Schwalm, R., *Progress in Organic Coatings* **2000**, *39*, 115-126.
15. Decker, C., Zahouily, K., Keller, L., Benfarhi, S., Bendaikha, T., Baron, J., *Journal of Materials Science* **2002**, *37*, 4831-4838.
16. Benfarhi, S., Decker, C., Keller, L., Zahouily, K., *European Polymer Journal* **2004**, *40*, 493-501.

17. Keller, L., Decker, C., Zahouily, K., Benfarhi, S., Le Meins, J.M., Mische-Brendle, J., *Polymer* **2004**, *45*, 7437-7447.
18. Shemper, B.S., Morizur, J.F., Alirol, M., Domenech, A., Hulin, V., Mathias, L.J., *Journal of Applied Polymer Science* **2004**, *93*, 1252-1263.
19. Uhl, F.M., Davuluri, S. P., Wong, S. C., Webster, D. C., *Polymer* **2004**, *45*, 6175-6187.
20. Decker, C., Keller, L., Zahouily, K., Benfarhi, S., *Polymer*, **2005**, *46*, 6640-6648.
21. Fogelstrom, L., Antoni, P., Malmstrom, E., Hult, A., *Progress in Organic Coatings* **2006**, *55*, 284-290.
22. Uhl, F.M., Webster, D. C., Davuluri, S. P., Wong, S. C., *European Polymer Journal* **2006**, *42*, 2596-2605.
23. Wang, Y.Y., Hsieh, T.E., *Journal of Materials Science* **2007**, *42*, 4451-4460.
24. Wang, Z., Pinnavaia, T. J., *Chemistry of Materials* **1998**, *10*, 1820-1826.
25. Wang, Z., Pinnavaia, T. J., *Chemistry of Materials* **1998**, *10*, 3769-3771.